Chemical Physics Letters 496 (2010) 356–361

Contents lists available at ScienceDirect

Chemical Physics Letters

journal homepage: www.elsevier.com/locate/cplett

Control of chemical reactions using external electric fields: The case of the LiNC ⇌ LiCN isomerization

G.E. Murgida [a,b], D.A. Wisniacki [b], P.I. Tamborenea [b], F. Borondo [a,c,*]

[a] Departamento de Química, Universidad Autónoma de Madrid, Cantoblanco, 28049 Madrid, Spain
[b] Departamento de Física 'J.J. Giambiagi', FCEN, Universidad de Buenos Aires, Pabellón 1, Ciudad Universitaria, C1428EHA Buenos Aires, Argentina
[c] Instituto Mixto de Ciencias Matemáticas CSIC-UAM-UC3M-UCM, Universidad Autónoma de Madrid, Cantoblanco, 28049 Madrid, Spain

ARTICLE INFO

Article history:
Received 3 May 2010
In final form 16 July 2010
Available online 21 July 2010

ABSTRACT

We explore the applicability to manipulate chemical reactions of a particularly simple method of quantum control that has been recently proposed in the literature [1]. For this purpose we use a realistic model for the isomerization of LiNC.

1. Introduction

Quantum control is a discipline of great current interest in science and engineering due to potential applications in many areas, including nanotechnology [1], quantum information processing [2], and chemical dynamics and reactivity [3–15]. The goal of quantum control is the external manipulation of a quantum system in order to bring it from the initial state to a desired, or target, final state.

Recently, some of us proposed a simple quantum control strategy [1,16–18], based on the knowledge of the variation of the spectrum of a system as a function of an external (control) parameter. The applicability of this method relies on the assumption that the energy spectrum of the system consists of a set of fairly isolated adiabatic curves which only interact in well-defined avoided crossing (ACs). Moreover, as the control parameter is swept across each AC the system should evolve as a two-level Landau–Zener system [19,20] for the strategy to work optimally. These two conditions may appear at first sight too restrictive but, as will be seen in this Letter, the method is quite general and it can be applied to a wide range of systems. In our previous work [1,17], the procedure was applied to a double quantum dot containing two interacting electrons using an external electric field as the control parameter. By using sequences of variations of the electric field, inducing diabatic and adiabatic passages through the existing ACs, the feasibility to travel through the energy spectrum connecting distant eigenstates was successfully demonstrated. This technique is also able to control the spatial localization of the electrons, opening the possibility to build coherent superpositions of eigenstates, thus constructing Bell's states, as described in Ref. [16].

In this work we explore the applicability of this control method to chemical reactivity. Many strategies have been described in the past for this purpose; see Refs. [3–15] and the references they contain. Most of them are based on optical strategies, relying on the high efficiency found in the modern laser technology. In particular, they usually take advantage of the ability to create and shape pulses even in the femtosecond scale or use interference between real dipole transitions. Among them, the dynamical Stark control method experimentally demonstrated by Sussman et al. [14] is somehow similar in spirit to the method proposed here. These authors modified the reaction probabilities in the dissociation of IBr by manipulating an AC existing in the electronic molecular potentials by means of an intense non-resonant laser pulse. In our proposal, however, one navigates through the ACs created by the external control parameter in the associated vibrational spectrum.

We choose to study isomerization reactions for their theoretical interest [21] and practical importance in many relevant chemical processes, specially of biological interest [22–25]. For example, the control of the HCN isomerization was thoroughly studied from the theoretical point of view [26–28], and the importance of intermediate states with configurations far from the usual ones discussed. Here we use a similar example, namely the LiNC ⇌ LiCN reaction, to illustrate our ideas. This system has been extensively studied in the past, specially in connection with the issue of quantum chaos in molecular system [29]. Similarly to the HCN molecule, the LiNC/LiCN isomerizing system has two linear stable configuration: the LiNC, which is the most stable one, and the LiCN. Our aim is to isomerize the molecular system, thus carrying it from the LiNC ground state configuration to LiCN. The controlling external field will be also a uniform electric field as in our previous study.

The Letter is organized as follows. In the next section we introduce the LiCN/LiCN molecular system and the model used in our calculations. Section 3 focusses on the control strategy that we design to manipulate the LiNC ⇌ LiCN isomerization; in it the

* Corresponding author at: Departamento de Química, Universidad Autónoma de Madrid, Cantoblanco, 28049 Madrid, Spain.
E-mail address: f.borondo@uam.es (F. Borondo).

0009-2614/$ - see front matter © 2010 Elsevier B.V. All rights reserved.
doi:10.1016/j.cplett.2010.07.057

corresponding theoretical methods and calculations are also described. In Section 4 we present and discuss our numerical results. Finally, the conclusions of the present study are summarized in Section 5. Notice that atomic units are used throughout the Letter, even for lengths and masses, unless otherwise stated.

2. The LiNC/LiCN molecular system

Let us next describe the theoretical model that will be used in this Letter to study the vibrational motion of the system that we intend to control quantum mechanically. The reaction that we have chosen to study is that for the LiNC/LiCN isomerizing molecular system. This molecule is representative of a large class of small polyatomic molecules, which exhibit similar behavior mainly due to the existence of a large amplitude (floppy) motion in one of the vibrational modes. This class includes different cyanides, such as HCN/HNC [30], alkaline cyanides [31], methylcyanide (CH_3CN) [32], and other similar species, including HCP [33,34], the HO_2 radical [35], or van der Waals complexes [36].

In LiNC/LiCN, the C and N atoms are strongly bounded by a triple covalent bond, while the Li is attached to the CN moiety by mostly ionic forces, due to the large charge separation existing between them. For these reasons, the CN vibrational mode effectively decouples from the other degrees of freedom of the molecule, and it can be considered frozen at its equilibrium value, $r_e = 2.186$. On the other hand, the relative position of Li with respect to the center of mass of the CN is much more flexible. In particular the bending along the angular coordinate is very floppy, and the corresponding vibration performs very large amplitude motions even at moderate values of the excitation energy. Accordingly, the vibrations of the whole system can be adequately described by the following 2° of freedom rotationless ($J = 0$) Hamiltonian

$$H_{\mathrm{LiCN}} = \frac{P_R^2}{2\mu_1} + \frac{1}{2}\left(\frac{1}{\mu_1 R^2} + \frac{1}{\mu_2 r_e^2}\right) P_\vartheta^2 + V(R,\vartheta), \tag{1}$$

where R and ϑ are the Jacobi coordinates specifying the position of the Li with respect to the center of mass, O, of the CN. P_R and P_ϑ are the associate conjugate momenta, and the corresponding reduced masses are given by $\mu_1 = m_{\mathrm{Li}} m_{\mathrm{CN}}/(m_{\mathrm{Li}} + m_{\mathrm{CN}}) = 10072$ and $\mu_2 = m_{\mathrm{C}} m_{\mathrm{N}}/m_{\mathrm{CN}} = 11780$.

The potential interaction, $V(R,\vartheta)$, is given by a 10-terms expansion in Legendre polynomials,

$$V(R,\vartheta) = \sum_{\lambda=0}^{9} v_\lambda(R) P_\lambda(\cos\vartheta), \tag{2}$$

where the coefficients, $v_\lambda(R)$, are combinations of long and short-term interactions whose actual expressions have been taken from the literature [37]. This potential, which is shown in Fig. 1 as a contour plot, has a global minimum at $(R,\vartheta) = (4.349, \pi)$, a relative minimum at $(R,\vartheta) = (4.795, 0)$, and a saddle point at $(R,\vartheta) = (4.221, 0.292\pi)$. The two minima correspond to the stable isomers at the linear configurations, LiNC and LiCN, respectively. The LiNC configuration, $\vartheta = \pi$, is more stable than that for LiCN, $\vartheta = 0$. The minimum energy path connecting the two isomers has also been plotted superimposed in Fig. 1 with dashed line.

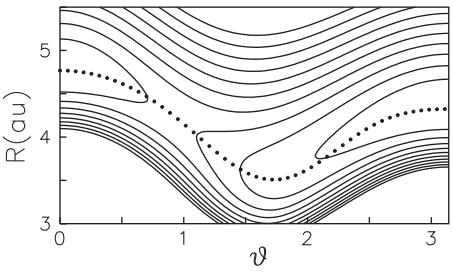

Fig. 1. Potential energy for LiNC/LiCN. The minimum energy path connecting the two isomers LiNC and LiCN has been plotted as a dashed curve.

Using the discrete variable representation method, as implemented by Bačić and Light [38], we calculate the first 900 eigenstates of Hamiltonian (1). (Only the first ~40 low lying states will be necessary for the discussions presented in this Letter.) The wave functions, $|n\rangle$, of the lowest lying eigenstates are localized in the $\vartheta = \pi$ well, and, therefore, correspond to the more stable configuration, LiNC. As higher energy levels are considered, the associated wave functions continue to be centered around $\vartheta = \pi$, but spread out along the minimum energy path. Actually, the first 30 levels correspond to LiNC structures, presenting an increasing number of nodes along the minimum energy path [39,40]. However, when one arrives at the 31st state the corresponding eigenfunction presents a LiCN structure, being localized around $\vartheta = 0$. Higher states, from $n = 32$ to $n = 39$ are again of the LiNC type, until state number 40, which is the first excited state of the LiCN type. Other higher excited LiCN states are, for example, n = 47, 52, 58, 64, 76, 80, 88, or 96. A more detailed description of this sequence along with an extended discussion on the dynamical characteristics of the LiNC/LiCN vibrational states can be found in Ref. [41].

3. Control of the LiNC ⇌ LiCN isomerization

In this Section, we describe the mechanism proposed in this work to control chemical reactions, also introducing the corresponding mathematical model for our case study: LiNC ⇌ LiCN. As indicated in the Introduction, several schemes have been already described in the literature aiming at the control of chemical reactivity.

In this Letter, we propose a very practical and simple alternative, consisting on the application of an external time-dependent electric field as the control parameter. As an example, we will illustrate this method by applying it to induce the isomerization LiNC ⇌ LiCN. The method is simple. By changing the intensity of an external electric field at a variable speed, the system can be made to 'navigate' in the correlation diagram of vibrational energy levels going from the initial state, usually the ground state, to the final desired one.

The mathematical model is also simple. Within the dipole approximation, the Hamiltonian describing the LiNC/LiCN molecular system in the presence of an external uniform electric field, $\vec{E}$, is given by

$$H = H_{\mathrm{LiCN}} + \vec{d}_{\mathrm{LiCN}}(R,\vartheta)\cdot\vec{E}, \tag{3}$$

where H_{LiCN} is the molecular Hamiltonian (without electric field) and $\vec{d}_{\mathrm{LiCN}}(R,\vartheta)$ is the corresponding dipole function. In order to simplify our model, we will further assume that:

(i) the molecule can be considered as an electric dipole with the negative charge located on the center of mass of the CN fragment and the positive charge on the Li [42],
(ii) we have a complete separation of charges, i.e. the dipole consists of a negative unit charge on the CN and a positive unit charge on the Li,
(iii) the electric field is assumed to be aligned with the CN bond, and
(iv) we assume that the isomerization process is fast compared with the rotation of the molecule.

Let us remark that the simplifying assumption (iii) is very much in the spirit of the molecular alignment techniques [43–45] and molecular rotation control [46], and certainly related with the

approximation (iv), that although not immediately obvious it has been checked by us [47] in the conditions of the present work. Introducing these approximations into Eq. (3), one finally obtains

$$H = H_{\mathrm{LiCN}}(R, \vartheta, P_R, P_\vartheta) + ER\cos\vartheta. \quad (4)$$

The eigenstates for the corresponding Hamiltonian operator are then obtained by direct diagonalization in the basis set of $\{|n\rangle\}$, considering E as a varying parameter. In this way the eigenenergies (correlation diagram) and eigenfunctions, $\{\phi_i\}$, for the states of LiNC/LiNC when the external field is applied are obtained.

4. Results

4.1. Correlation diagram

We show in the bottom part of Fig. 2 the correlation diagram of vibrational energy levels as a function of the intensity of the external electric field (along the N–C direction) for the LiNC/LiCN isomerizing system. Since all involved states are of the same symmetry, the Wigner–von Neumann non-crossing rule [48] applies. According to it, when two such states evolve as a function of an external parameter, the intensity of the electric field in this case, the corresponding energy curves may eventually get very close, but due to this rule they cannot cross. As a result we have an AC in the correlation diagram. In the range of parameter values where this happens, some mixing of the corresponding wavefunctions takes place, according to the model developed independently by Landau [19] and Zener [20]. This mixing can be eliminated by means of a suitable transformation. The new states obtained in this way are called diabatic [49], and they do cross at the same point where the AC (in the adiabatic representation) is located.

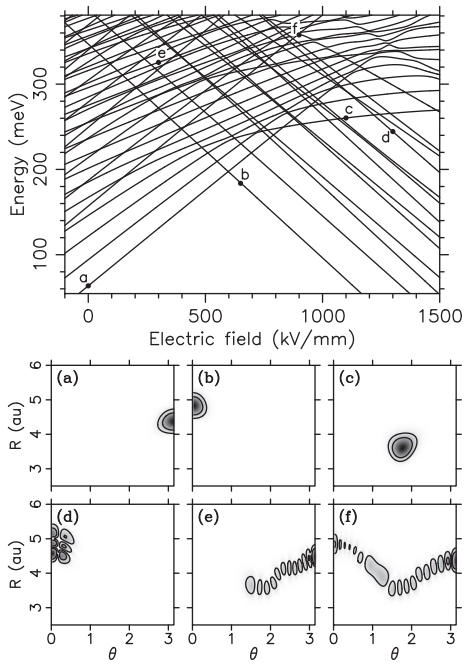

Fig. 2. (top) Correlation diagram for the vibrational energy levels of LiNC/LiCN as a function of the intensity of an external electric field along the N–C direction. The curves with more pronounced slope are associated to states localized on either of the two linear isomer configurations. Positive slopes corresponding to LiNC and negative to LiCN. The curves with lower (absolute) value of the slope represent isomerizing states. (bottom) Wave functions for the eigenstates at different points in the correlation diagram. Their structures correspond to: (a) ground state in the LiNC well, (b) ground state in the LiCN well ($n = 31$ in the absence of electric field), (c) state localized between the two wells, (d) excited state in the LiCN well ($n = 10$) in the absence of electric field, (e) excited state in the LiNC well ($n = 21$ in the absence of electric field), and (f) isomerizing state at an avoided crossing.

As can be seen, many of these ACs exist in our spectrum of Fig. 2, their positions indicating the values of E at which there is an interaction among some of the eigenstates of the full Hamiltonian (Eq. (4)). Moreover, it is observed that the spectrum consists mostly of straight diabatic lines, with either positive or negative slopes, plus some other curves with visibly smaller inclinations. This behavior is easily understood. Each straight line corresponds to an eigenstate whose character does not change significantly in the range of electric field intensities that we are considering. In particular, their electronic structures, and consequently their dipole moments, do not change much. Moreover, the energy curves corresponding to states located in the LiNC, which have positive values of this magnitude, will be practically straight lines with a positive slope in the correlation diagram. The opposite is true, on the other hand, for states located on the other isomer well, LiCN. In both cases, the slopes coincide with the mean dipole moment, given by $d_i = \langle\phi_i|R\cos\vartheta|\phi_i\rangle$ in our case (see Eq. (4)). Finally, there are also states with completely different characteristics, hybrid between the two isomeric structures, such as the isomerizing states which are delocalized all along the whole minimum energy path [41]. These states present intermediate values on their inclinations. To further illustrate these effects, we have marked different relevant points, (a)–(f), in the correlation diagram of Fig. 2, and plotted the corresponding wave functions in the top panel. As can be seen, states at points (a) and (e) are localized in the LiNC well, with structures corresponding to the ground and $n = 21$ (in the absence of electric field) states, respectively. Points (b) and (d), on the other hand, correspond to states (ground and excited on the other isomer, LiCN; point (f), which is at the middle of an AC, indicates the presence of isomerizing states; and finally, point (c) corresponds to an uncommon structure, only possible due to the presence of the external electric field, for which the probability density accumulates in an intermediate point along the minimum energy path.

4.2. Controlling isomerization

Let us consider now how the isomerization LiNC $\rightleftharpoons$ LiCN can be controlled by just adjusting in appropriate way an external electric field within a given time interval. As an example, we will concentrate on a path taking our molecule from its ground state (in the absence of the electric field), LiNC, to an eigenstate corresponding to the LiCN isomer. This will be done without ever leaving the adiabatic curves in our correlation diagram, i.e. being all the time in eigenstates of the system plus electric field [Eq. (4)].

As stated above, the basic idea of our method of control consists of navigating the correlation diagram of the LiNC/LiCN using their energy curves as suitable channels. We start by changing the magnitude of the electric field slowly enough to move adiabatically on the starting curve. When this curve approach an AC we decide whether we want to stay in it, or we prefer to 'jump' to the crossing state. In the first case, we will perform an adiabatic transition at the AC, while in the second we need to transverse the AC diabatically. In this way, we continue using the ACs in the correlation diagram as bifurcations points on our path. This allows to navigate the spectrum in many different ways, just by choosing between the different branches at the encountered ACs, until the final desired destination point is reached.

According to the Landau–Zener theory, a rapid change of the parameter produces at an AC a jump between the involved energy levels, i.e. a diabatic crossing of the AC, while a slow change leaves the system in the same energy level, i.e. adiabatic change. In the latter case, the crossing of the AC produces a change in the wave function of the state, and then in its physical characteristics, such

as the dipole moment. Moreover, this theory can be used quantitatively to estimate the rate of change on the electric field necessary to induce diabatic or adiabatic transitions at any given AC in our system. Namely, assuming that the evolution of the system can be described in the neighborhood of the AC with just a two-level model, and the parameter is varied at a constant rate, we have that the (diabatic) transition probability between the two involved states, i and j, is given by

$$P_{i\to j} = 1 - \exp\left(-\frac{\pi\Delta^2}{2\hbar|d_i - d_j|\dot{E}}\right), \tag{5}$$

where d_i and d_j are the slopes of the diabatic straight lines [approximated to a very good approximation by the dipole moment of the molecule, see Eq. (3)], Δ is the energy gap at the AC, and $\dot{E}$ the parameter velocity. It can be easily seen that if $\dot{E} \ll \pi\Delta^2/(2\hbar|d_i - d_j|)$, we have an adiabatic transition, while when $\dot{E} \gg \pi\Delta^2/(2\hbar|d_i - d_j|)$, a diabatic transition takes place.

4.3. Control strategies

Now, by careful examination of the vibrational energy levels of LiNC/LiCN we can design different possible strategies to isomerize the molecule. For example, the simplest way to induce the desired reaction is to go directly from point a to point b marked in Fig. 2 (see the shape of the corresponding wave functions in the top part of the figure). As can be seen, this involves increasing the electric field until encountering the first AC, and then adiabatically passing through it. This can be accomplished if the variation of the applied electric field is very slow. However, the gap at the AC between these two levels is extremely small, and therefore the time needed to cross it adiabatically is far too large for all practical purposes. Indeed, considering that $\Delta = 0.00002$ mEV and $|d_i - d_j| = 0.5$ meV/(kV/mm), in this case, one obtains $\dot{E} \ll 2000$ (kV/mm)/s, which is negligibly slow. Notice that this is so because the wave functions of the involved (diabatic) states are localized in very disjoint regions. And the same is true for all other ACs involving LiNC and LiCN states, thus preventing the possibility of isomerization via a single adiabatic crossing.

One possibility to overcome this problem is isomerize the molecule passing through an intermediate state of the hybrid type described above. With this strategy in mind, we have designed the control path marked with arrows in the correlation diagram of Fig. 3, which takes the molecule from the LiNC ground state level, marked with a full square on the figure, to a LiCN excited state, marked with a crossed circle. As we will see below, using this alternative the isomerization can be fully performed in just 450 ps. To help in the discussion six vertical dashed lines at $E = E_1, \ldots, E_6$, respectively, have also been plotted in the figure.

Let us continue by describing in more detail how this path should be implemented in order to induce the desired isomerization LiNC ⇋ LiCN. As can be seen in Fig. 3, the crucial points are: First, the intensity of the external field has to be increased in such a way that the system remains in the ground state structure (LiNC), by diabatically traversing across the ACs with the first low lying LiCN states (straight lines with negative slopes in the correlation diagram). Second, make the system to evolve adiabatically to a hybrid state, ϕ_{12}, when the field intensity reaches the AC at $E = E_3$. And third, make a second adiabatic transition at $E = E_5$, keeping the system in the ϕ_{15} state which has the desired LiCN character, to finish at $E = E_6$ in the target point marked with a cross circle in the correlation diagram of Fig. 3. To induce these processes one has to vary the applied external field at specific rates, that are evaluated with the aid of Eq. (5), in order to achieve a square modulus of the overlap between the final state and the target one equal to 0.99.

The field variation as a function of the elapsed time computed in this way is shown at the top panel of Fig. 4. Here we see that the resulting function consists of several linear pieces, i.e. the intensity of the field is kept constant except at some instants of time, when it is suddenly varied. Also, the instants of time, $t_1, \ldots, t_6$, corresponding to the points $E_1, \ldots, E_6$ in the correlation diagram of Fig. 3, have been marked with vertical dashed lines. As can be seen in Fig. 3, as the electric field is increased our selected path first consists of a diabatic evolution through the first eleven ACs. All of them can be easily crossed by increasing suddenly the electric field. However, in order to stay all the time on the adiabatic curve corresponding to the first LiNC, the speed of the electric field must be sufficiently slow. Among these crossings, the first four correspond to LiNC → LiCN transitions and then they can be easily

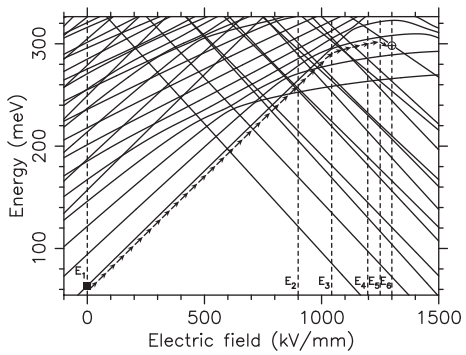

Fig. 3. Schematic plot of the intended path in order to reach a LiCN state. This path include two adiabatic transitions inducing the isomerization through an intermediate state with hybrid dynamical characteristics. See text for details.

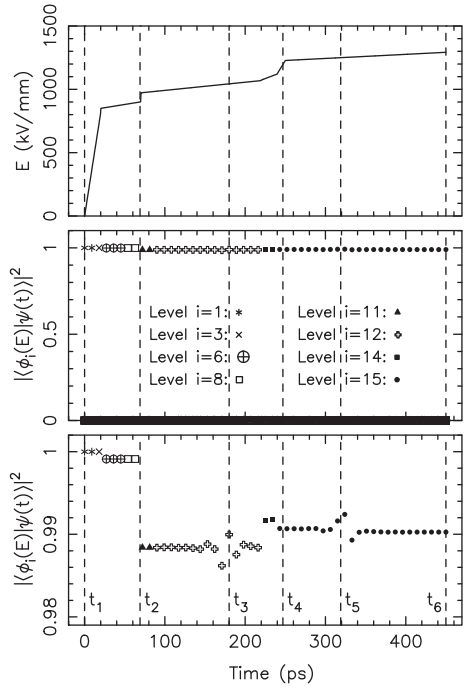

Fig. 4. (top) Time variation of the applied external electric field intensity used to induce the LiNC ⇋ LiCN isomerization along the path marked with arrows in Fig. 3. (middle) Time evolution of the population on selected states in the correlation diagram of Fig. 3 computed as the square overlap of the total wave function (6) with the eigenstates, ϕ_i, of Hamiltonian (4). (bottom) Blow up of the upper part of the middle panel, showing in more detail the probability of the most populated states. As can be seen the target state is reached with a probability greater than 0.99.

crossed diabatically if a very low field speed is used. For example, by increasing the field from $E = 0$ to 813.3 kV/mm in 20 ps, as shown in the top panel of Fig. 4. Next, the system encounters the fifth AC, taking place at $E = 832.3$ kV/mm. Here, two levels both with positive slopes and a larger magnitude of the gap (not appreciable in the scale of the figure), thus requiring a larger value of $\dot{E}$ to cross it diabatically, are involved. To optimize the transition at this AC, we use an almost instantaneous jump in intensity of the field, increasing it up to $E = 849.7$ kV/mm. This jump is an almost vertical transition, barely visible in the scale of the figure, at the end of the first straight line. Afterwards, the field is further increased at a smaller rate reaching $E = 901.1$ kV/mm in 50 more picoseconds. In this way, we arrive at $t = t_2$ (E_2 in Fig. 3), having crossed two more ACs and being the system wave function $\psi(t_2) = \phi_8$. Now we are facing the eighth AC, that again involves two states with dipoles of the same sign, and requires accordingly a faster rate of change in the electric field. This is accomplished by abruptly passing from $E_2 = 901.1$ kV/mm to 972.3 kV/mm. As the ACs number 9, 10, and 11 are much narrower, this value of speed also allows to cross them diabatically in this same period. Then, the first adiabatic evolution, taking the system at t_3 to the intermediate hybrid state ϕ_{12}, is induced by taking the field from 972.3 kV/mm to 1069.0 kV/mm in 150 ps. Next, a diabatic transition through the last three ACs is accomplished by changing the field in two steps: first, to 1121.0 kV/mm in 20 ps, and then to 1227.8 kV/mm in 10 ps, thus taking the system to $\psi(t_4) = \phi_{15}$. Finally, we have an adiabatic evolution in the last AC at t_5, the intensity of the field is increased slowly from 1227.8 kV/mm to 1292.4 kV/mm in 200 ps, landing in the desired isomerized LiCN structure. One point of practical importance is worth commenting here. The high values of the fields appearing in our calculations are not unusually high, since they are of the magnitude of those currently presently used in some electrochemical applications (see for example [50]), but the ramping variations required may still represent a challenge for the existing technologies, that hopefully can be overcome in a near future.

This description can be made quantitative by monitoring the associated state evolution, this also giving the evolution of the populations in the correlation diagram. For this purpose, we use a fourth-order Runge–Kutta method to numerically integrate the corresponding time-dependent Schrödinger equation, $-i[\partial\psi(t)/\partial t] = \hat{H}(t)\psi(t)$, with the time-dependent electric field profile shown in the top panel of Fig. 4. In this way, the coefficients in the adiabatic basis set,

$$\psi(t) = \sum_i a_i(t)\ \phi_i[R, \vartheta; E(t)], \tag{6}$$

are obtained (see Eq. (6)). As the initial state we take the ground state when no electric field is applied (LiNC), i.e. $a_1(0) = 1$ and $a_{i\neq 1}(0) = 0$. The results for some relevant eigentates, ϕ_i, are shown in the middle panel of Fig. 4. In it, the population jumps among the different fifteen eigenstates, but being very close to unity at all times. Actually, in the blow up on the bottom panel of the figure, we can check that these populations never go below $|a_i(t)|^2 = 0.99$.

The corresponding shape of the system wavefunction, $\psi(t)$, at different times during the evolution is shown in Fig. 5. As can be seen, the process is started from the ground state of LiNC without electric field at $t_1 = 0$. Later, at $t_2 = 69$ ps, the state remained with the same vibrational structure, although the corresponding wavefunctions had changed a little bit due to the effect of the controlling external field. The first adiabatic transition takes place around $t_3 = 180$ ps, where the probability density localized around $\vartheta = \pi$ starts to leak importantly into a hybrid structure centered at intermediate values of ϑ. This structure is clearly defined at $t_4 = 247$ ps. As the control process continues, and the electric field

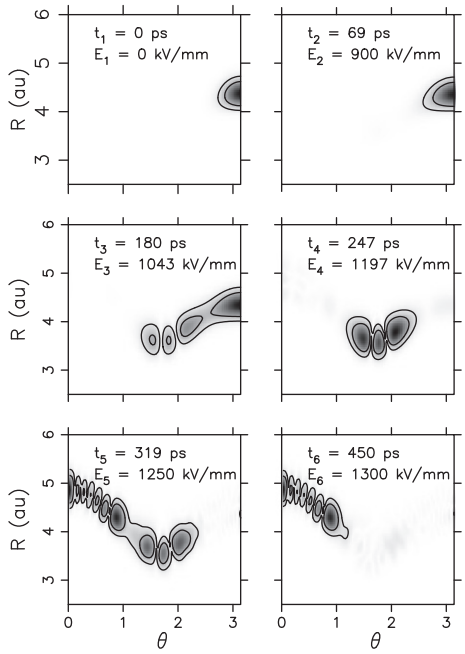

Fig. 5. Time evolution of the system wavefunction, $\psi(t)$, along the controlled isomerization process.

is increased, we get around $t_5 = 319$ ps to the second adiabatic transition, allowing us to reach finally the desired excited LiCN structure at $t_6 = 450$ ps.

By continuing this process in a similar way we could redirect our state to other situations, for example to the lowest LiCN state with no field applied.

5. Conclusions

In this Letter we have examined the possibility of using a very simple method, originally proposed in connection with nanotechnological devices, to control and manipulate chemical reactions. The idea consists of applying an external electric field which is made to vary at specific rates in order to navigate the corresponding state correlation diagram. In this way the system can be taken from an initial state, usually the ground state, to another one with different properties, making it to traverse the different ACs in the correlation diagram in the appropriate way.

In our case we have chosen the isomerization reaction LiNC $\rightleftharpoons$ LiCN to illustrate the method. The reason for this choice is twofold. First it allows the use of many simplifications and approximations that made the calculations simple. Recall that the main aim of the Letter is to show the feasibility of the method rather than to present a specific application. Second, this system shows a very rich variety of vibrational motions and serves as a prototype of many similar molecules and dynamical processes of chemical interest.

Acknowledgements

Support from MICINN-Spain (MTM2009-14621 and i-MATH CSD2006-32), and CONICET-Argentina (PIP-6137 and No. PIP-5851), and UBACyT-Argentina (X237 and No. X495) is gratefully acknowledged. DAW and PIT are researchers at CONICET-Argentina.

References

[1] G.E. Murgida, D.A. Wisniacki, P.I. Tamborenea, Phys. Rev. Lett. 99 (2007) 036806.
[2] D. D'Alessandro, Introduction to Quantum Control and Dynamics, Chapman and Hall/CRC Applied Mathematics Nonlinear Science, 2007.
[3] A. Assion et al., Science 282 (1998) 919.
[4] T. Brixner, N.H. Damrauer, P. Nicklaus, G. Gerber, Nature 414 (2001) 57.
[5] S.A. Rice, M. Zhao, Optical Control of Molecular Dynamics, Wiley, New York, 2000.
[6] S.M. Hurley, W. Castleman Jr., Science 292 (2001) 5.
[7] A.D. Bandrauk, Y. Fujimura, R.J. Gordon, Laser Control and Manipulation of Molecules, ACS Symposium Series, vol. 821, American Chemical Society, Washington, DC, 2002.
[8] M. Shapiro, P. Brumer, Principles of the Quantum Control of Molecular Processes, Wiley-VCH, Weinheim, 2003.
[9] R.J. Levis, G.M. Menki, H. Rabitz, Science 292 (2001) 709.
[10] H. Rabitz, Science 299 (2003) 525.
[11] R. Chakrabarti, H. Rabitz, Int. Rev. Phys. Chem. 26 (2007) 671.
[12] H. Niikura, F. Légaré, R. Hasbani, A.D. Bandrauk, M.Y. Ivanov, D.M. Villeneuve, P.B. Corkum, Nature 417 (2002) 917.
[13] H. Niikura, P.B. Corkum, D.M. Villeneuve, Phys. Rev. Lett. 90 (2003) 203601.
[14] B.J. Sussman, D. Townsend, M. Yu. Ivanov, A. Stolow, Science 314 (2006) 278.
[15] V.S. Letokhov, Laser Control of Atoms and Molecules, Oxford University Press, Cambridge, 2007.
[16] G.E. Murgida, D.A. Wisniacki, P.I. Tamborenea, Phys. Rev. B 79 (2009) 035326.
[17] D.A. Wisniacki, G.E. Murgida, P.I. Tamborenea, AIP Proc. 963 (2007) 840.
[18] G.E. Murgida, D.A. Wisniacki, P.I. Tamborenea, J. Mod. Opt. 56 (2009) 799.
[19] L. Landau, Phys. Sov. Union 2 (1932) 46.
[20] C. Zener, Proc. R. Soc. Lond. A 137 (1932) 696.
[21] T. Baer, W.H. Hase, Unimolecular Reaction Dynamics: Theory and Experiments, Oxford University Press, Oxford, 1996.
[22] G. Vogt, G. Krampert, P. Niklaus, P. Nuernberger, G. Gerber, Phys. Rev. Lett. 94 (2005) 068305.
[23] B. Dietzek, B. Brüggemann, T. Pascher, A. Yartsev, Phys. Rev. Lett. 97 (2006) 258301.
[24] V.I. Prokhorenk, A.M. Nagy, S.A. Waschuk, L.S. Brown, R.R. Birge, R.J. Dwayne Miller, Science 313 (2006) 1257.
[25] T.T. To, E.J. Heilweil, R. Duke III, K.R. Ruddick, C.E. Webster, T.J. Burkey, J. Phys. Chem. A 113 (2009) 2666.
[26] B.L. Lan, J.M. Bowman, J. Chem. Phys. 101 (1994) 8564.
[27] W. Jakubetz, B.L. Lan, Chem. Phys. 217 (1997) 375.
[28] S.P. Shah, S.A. Rice, J. Chem. Phys. 113 (1999) 15.
[29] F. Borondo, R.M. Benito, in: F. Khanna, D. Matrasulov (Eds.), NATO Science Series II, vol. 213, North-Holland, Dordrecht, 2006, p. 115.
[30] J.N. Murrell, S. Carter, L.O. Halonen, J. Mol. Spectrosc. 93 (1982) 307.
[31] D.-K. Lee, I.S. Lim, Y.-S. Lee, D. Hagenbaum-Reignier, G.-H. Jeung, J. Chem. Phys. 126 (2007) 244313.
[32] A.J. Marks, J.N. Murrell, A.J. Stace, J. Chem. Phys. 94 (1991) 3908.
[33] H. Ishikawa, R.W. Field, S.C. Farantos, M. Joyeux, J. Koput, C. Beck, R. Schinke, Annu. Rev. Phys. Chem. 50 (1999) 443.
[34] Z.S. Safi, J.C. Losada, R.M. Benito, F. Borondo, J. Chem. Phys. 129 (2008) 164316.
[35] A.J.C. Varandas, J. Brandão, L.A.M. Quintales, J. Phys. Chem. 92 (1988) 3732.
[36] A. Gamboa, H. Hernández, J.A. Ramilowski, J.C. Losada, R.M. Benito, F. Borondo, D. Farrelly, Phys. Chem. Chem. Phys. 11 (2009) 8203.
[37] R. Essers, J. Tennyson, P.E.S. Wormer, Chem. Phys. Lett. 89 (1982) 223.
[38] Z. Bačić, J.C. Light, J. Chem. Phys. 85 (1986) 4594.
[39] F.J. Arranz, R.M. Benito, F. Borondo, J. Chem. Phys. 123 (2005) 044301.
[40] F.J. Arranz, R.M. Benito, F. Borondo, J. Chem. Phys. 120 (2004) 6516.
[41] F.J. Arranz, R.M. Benito, F. Borondo, J. Chem. Phys. 107 (1997) 2395.
[42] B. Bak, E. Clementi, R.N. Kortzeborn, J. Chem. Phys. 52 (1970) 764.
[43] B. Friedrich, D. Herschbach, Phys. Rev. Lett. 74 (1995) 4623.
[44] M. Leibscher, I. Sh. Averbukh, H. Rabitz, Phys. Rev. A 69 (2004) 013402.
[45] S. De et al., Phys. Rev. Lett. 103 (2009) 153002.
[46] S. Fleischer, Y. Khodorkovsky, Y. Prior, I. Sh. Averbukh, New J. Phys. 11 (2009) 105039.
[47] F.J. Arranz, R.M. Benito, G.E. Murgida, D.A. Wisniacki, P.I. Tamborenea, D. Farrelly, F. Borondo, in preparation.
[48] B.H. Bransden, C.J. Joachain, Quantum Mechanics, Pearson Prentice Hall, Harlow, 2000.
[49] F.T. Smith, Phys. Rev. 179 (1969) 111.
[50] D.H. Murgida, P. Hildebrandt, Acc. Chem. Res. 37 (2004) 854.